

POSITION ANALYSIS OF ROCK BURSTS IN THE AREA OF THE MAYRAU MINE SHAFT PILLAR

MILOŠ VENCOSKÝ

Institute of Rock Structure and Mechanics, Academy of Sciences of the Czech Republic
V Holešovičkách 41, 182 09 Prague 8, Czech Republic

In the area of the Mayrau Mine shaft pillar (Kladno Coal-Mining Area) foci of rock bursts, generated as a result of mining operations being carried out inside the pillar, have been monitored and localized since 1994. These foci can be localized due to the local seismic network, established in the area over recent years, and consisting originally of 9 seismic stations (Fischer, 1992), located on the surface (4 stations), as well as below the surface (5 stations). The rock bursts were monitored in an effort to discover the geometric relations between the mining operations and the occurrence of these bursts. The principal purpose of this research was to acquire knowledge which would enable the prediction of burst zones with regard to planned exploitation, and thus to contribute to the safety of mining operations in this mine.

1. INTRODUCTION

Only a few papers (Růžek; Málek, 1997), which are, however, slightly remote to the topic of this paper, have so far been published in this connection. Most closely related to this topic is paper (Buben and Vencovský, 1996) which presents a comprehensive review of the positions of the bursts in 1995 with respect to the exploitation being carried out in the Mayrau Mine shaft pillar. The cumulation of burst locations and their migration, if any, were derived in the paper from an analysis, the principles of which were formulated by the present author. The said analysis was founded on dividing the superposed volume, in which most bursts occur, into elementary cubes of identical dimensions, and on determining the absolute, or relative frequencies of the burst phenomena in the separate cubic elements. These frequencies were then assigned to the centres of these cubes whereby a spatial digital grid model of a scalar field was created. This model was then depicted in terms of isolines in conveniently selected plane sections running parallel with the planes of a rectangular spatial coordinate system. Based on this analysis, the authors of this paper arrived at several principal facts (Figs 1a, 1b, 1c).

- In the horizontal plane, the bursts accumulated in three zones: A, B, C. Zone A is the most active and, for practical purposes, does not change its position. Its burst activity clearly depends on the neighbourhood, where mine operations are being carried out to the north-west of the safety pillar. The behaviour, although

- less pronounced, of Zone C in the neighbourhood of the mining to the south-east of the pillar, is similar. Zone B has hitherto been but little seismically active.
- In terms of elevation, most of the bursts occur practically at the same level, i.e. at about 100 m below sea level, which is about 80 to 100 m above the mining operations, varying roughly over a range of 30 metres.
 - The positions of all three zones agrees to some extent with the positions of regions of maximum changes in horizontal and vertical motions, which can be identified by prediction calculations of the effects of subsidence with regard to the stope made in the pillar in 1995 and for the above level of most of the bursts (80 to 100 m above the stope level - Figs 1b, 1c). In this connection, one can arrive at a controversial finding that the positions of Zones A, B, C only correspond to those parts of the predicted regions which are located inside the shaft pillar. In the remaining, horizontally and symmetrically situated parts of these regions, located outside the pillar, only bursts with no tendency to accumulate are observed. This can be explained only hypothetically by the rock massif within the shaft pillar being to some extent still a compact and, therefore, fragile body, whereas the rock massif outside the pillar has been nearly completely disrupted by old mining operations, which have been going on there practically from the end of the last century, and, consequently, is able to react to the mechanical stress by fragile deformation but very little.

In connection with the analysis of quantified accumulation of bursts, mentioned above, it should be pointed out that this analysis yields only very generalized results, lacking detailed differentiation of the density distribution. Hence, the author has worked out a new, principally different method of analyzing the density distribution (Vencovský, 1996) and has used it in this study not only to analyze rock bursts, recorded in 1996 and in the first half of 1997, but also to re-analyze all 1995 bursts. The principal difference of this new method is in studying the position density of burst occurrence in the given region as a planar phenomenon, occurring in the horizontal plane only. The density at the point of a particular burst is defined in terms of the "average" distance of burst foci.

The respective results, to be described below, provide much better evidence of the positional dependence of burst occurrence on the exploitation works, and also enable other connections, concerning the nature of burst cumulation and global deformation of the rock massif within the scope of the shaft pillar, to be derived. Facts of this nature can be considered the primary contribution of this study.

An objective position analysis of the occurrence of burst foci with respect to any geometric relations requires the accuracy of localizing them on the basis of the initial time data to be derived. This accuracy is, to some extent, affected by the localization method used. Hence, the choice of the method is most important, because it can also provide important information about the velocities of seismic waves, as well as about the anisotropy and homogeneity of these velocities. Consequently, a substantial part of this paper will also be devoted to these problems, the proposed and applied solutions of which may be considered a further asset of this study.

In conclusion of the introductory section, a remark on the seismic network men-

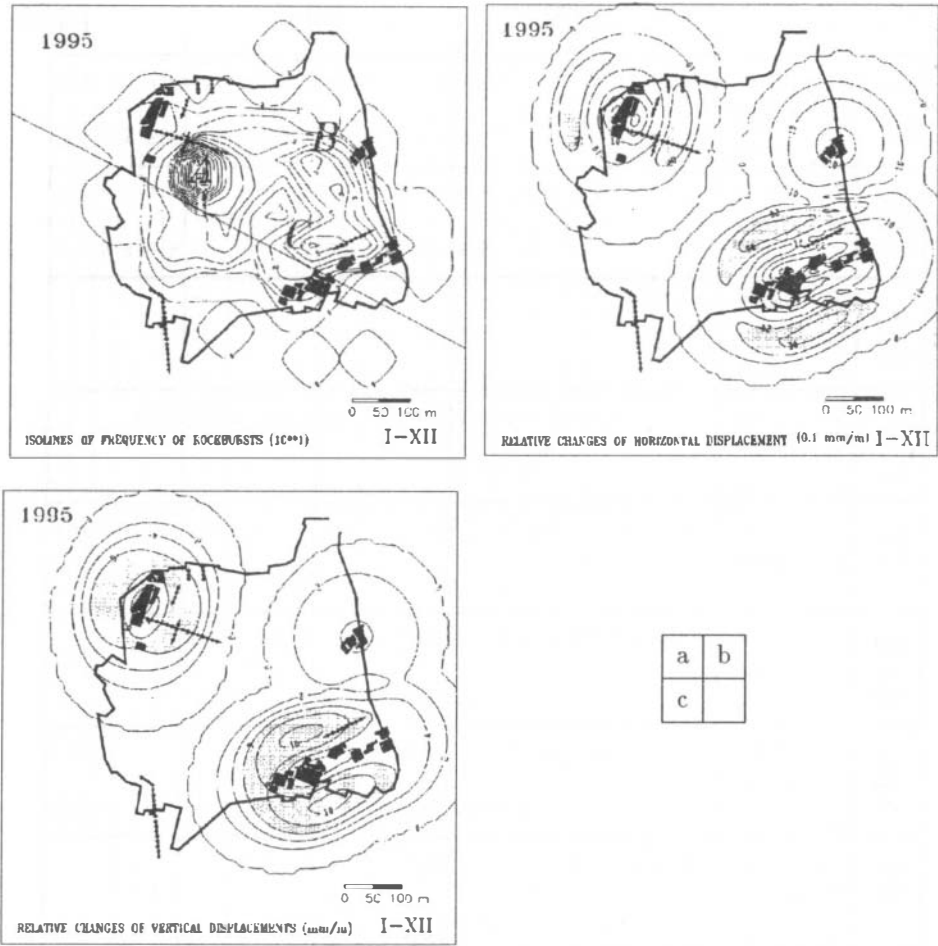


FIG. 1. a. Frequency distribution of rock bursts in 1995. The isolines are dimensioned in tens of bursts
 b. Prediction of absolute values of relative changes (mm/m) of horizontal motions at the level of -100 m for mining operations conducted in 1995. The isolines are dimensioned in tenths of mm/m
 c. Prediction of absolute values of relative changes (mm/m) of vertical motions at the level of -100 m for mining operations conducted in 1995. The isolines are dimensioned in tenths of mm/m

tioned above, which has undergone certain changes from the time it was established. These changes consisted in the gradual decommissioning of the individual stations

		1995										1996										1997																		
BYT	Y= 765578. X= 1030928. Z= 350.	P	P	P	P	P	P	P	P	P	P	P	P	P	P	P	P	P	P	P	P	P	P	P	P	P	P	P	P	P	P	P	P	P	P	P	P	P	P	
CEN	Y= 765539. X= 1031079. Z= 350.	P	P	P	P	P	P	P	P	P	P	P	P	P	P	P	P	P	P	P	P	P	P	P	P	P	P	P	P	P	P	P	P	P	P	P	P	P	P	
DES	Y= 765663. X= 1031013. Z= -167.	P	P	P	P																																			
DSP	Y= 765490. X= 1030953. Z= -167.					P	P	P	P	P	P	P	P	P	P	P	P	P	P	P	P	P	P	P	P	P	P	P	P	P	P	P						S		
GRZ	Y= 765429. X= 1031068. Z= 348.	P	P	P	P	P	P	P	P	P	P	P	P	P	P	P	P	P	P	P	P	P	P	P	P	P	P	P	P	P	P	P	P	P	P	P	P	P	P	
KAM	Y= 765580. X= 1031163. Z= -49.	P	P	P	P	P	P	P	P	P	P	P	P	P	P	P	P	P	P	P	P	P	P	P	P	P	P	P	P	P	P									
KRY	Y= 765672. X= 1031134. Z= 352.	P	P	P	P	P	P	P	P	P	P	P	P	P	P	P	P	P	P	P	P	P	P	P					P									P	P	P
SED	Y= 765548. X= 1031095. Z= -49.	P	P	P	P	P	P	P	P	P	P	P	P	P																										
TRE	Y= 765532. X= 1031047. Z= 201.	P	P	P	P	P	P	P	P	P	P	P	P	P	P	P	P	P	P	P	P	P	P	P	P	P	P	P	P	P	P	P	P	P	P	P	P	P	P	
PAT	Y= 765545. X= 1031051. Z= 98.	P	P	P	P	P	P	P	P	P	P	P	P																											

FIG. 2. Overview of the operation of the MAYRAU seismic network in 1995–1997.5.

which, as will be pointed out below, had a negative effect on the accuracy with which the bursts were localized. The following table gives the basic parameters and an account of the activity of the network.

A review of the activity of all 9 stations from 1995.1 to 1997.6 is shown in Fig. 2. The letters P and S refer to the station's activity in a particular month of the appropriate year, and also indicate whether the observer at the station evaluated the arrival times of P- or S-waves. Figure 2 shows that, in 1995, practically all 9 stations were active (station DES was relocated in May 1995 and subsequently designated as DSP), whereas at the beginning of 1997 only 4 stations were operating reliably, of which only station TRE was subsurface. Figure 3 provides a geometric idea of the distribution of these stations in the area of the shaft pillar.

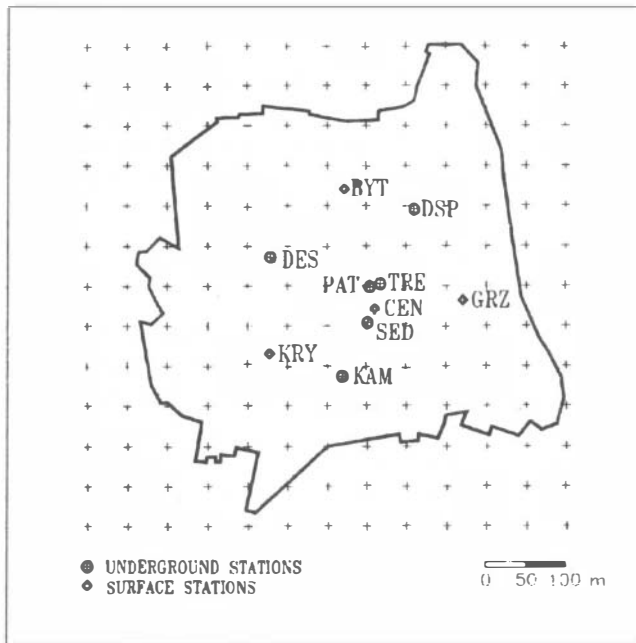


FIG. 3. Distribution of seismic stations

2. LOCALIZATION METHODS

By way of introduction, it should be pointed out that all formulations, hereinafter given, of the localization methods are based on the fundamental assumption of simplifying the properties of the rock environment which is considered to be a homogeneous rock body without velocity boundaries. Although this is a considerably simplifying assumption, it can be accepted for the given mining area based on previous experience.

The unknown spatial coordinates of the burst focus, x , y , z , of the focal time, t , and of some other parameters characterizing the velocity of propagation of seismic waves in a rock environment are derived from the arrival times of P- or S-waves, observed at $i = 1$ to n stations of the seismic network, whose coordinates are x_i ,

y_i, z_i . Various localization methods can now be used for this purpose. In principle, these methods can be divided into two groups (Šílený, 1987).

Classical methods, formulated on the basis of the condition of the least sum of squares of deviations vp_i, vs_i :

$$vp_i = tp_i - tp'_i, \quad vs_i = ts_i - ts'_i, \quad (1)$$

between the observed times tp'_i and ts'_i of the arrival of P- and S-waves and the corresponding times tp_i and ts_i , given by the analytical intermediary function

$$t_i = F(x, y, z, t, V, x_i, y_i, z_i), \quad (2)$$

in which the required unknowns x, y, z, t and the parameters of the rock environment occur; the most important of the latter is the velocity of propagation of seismic waves, V . These methods, which are based on the above condition of the "least sum of squares", m , of deviations, determined from Eq. (1),

$$\sum_{i=1}^m (vp_i vp_i + vs_i vs_i) = \min, \quad (3)$$

are formulated according to the principles of the calculus of observations, still frequently used to-day, whose historical founder was C.F. GAUSS (Jordan and Egger, 1920). In this particular connection, this method of adjustment was first used by Geiger (1912) (Šílený, 1987) to derive the 4 fundamental unknowns mentioned above. The reader should be reminded that the methods in this group enable only individual adjustment, i.e. deriving the said unknowns in each case for a set of observed times which refer only to a single particular burst. The number of time data, required to carry out this adjustment, i.e. the sum $tp_i + ts_i$, must always be larger than the number of unknowns to be determined. The advantage of these methods is the very fast numerical solution.

Tomographic methods (Málek, 1997; Šílený, 1987) which enable a number of burst foci to be localized at one time without invoking the principles of the classical calculus of observations. These methods, such as the Monte Carlo method, simplex method, gradient method, isometric method, are founded on the direct minimization of the sum of functions (3) which can be defined for a particular group of bursts, and which lead up to deriving the burst foci in the group, as well as to determining the seismic velocities, characteristic for the rock environment. These properties also gave these methods their name. Their disadvantage is the rather time-consuming numerical solution, increasing non-linearly with the number of bursts in the group being treated (Málek, 1997).

Into the automated system of the local seismic network at the Mayrau Mine, called SEISBASE (Fischer and Hampl, 1997), the authors of this system inserted the simplex method, which yields the four fundamental unknowns mentioned above, assuming constant velocities of P-waves and S-waves

$$V_p = 2185 \text{ m/s}, \quad V_s = 1090 \text{ m/s}. \quad (4)$$

These velocities were studied in (Málek, 1997) using tomographic methods for the homogeneous isotropic model mentioned above, as well as for a homogeneous model with a simply continuously defined anisotropy. The study was conducted in a group of 29 bursts selected so that they were as far away from one another as possible. For the homogeneous isotropic velocity model of the medium the author derived velocities

$$V_p = 2220 \text{ m/s}, \quad V_s = 1060 \text{ m/s}, \quad (5)$$

and for the homogeneous anisotropic model the author arrived at

$$V_h = 2660 \text{ m/s}, \quad V_v = 1960 \text{ m/s}, \quad (6)$$

having taken the velocity of P-waves, V_p , in the direction deflected from the vertical by angle G , to be given by the equation

$$V_p^2 = V_v^2 \cos^2 G + V_h^2 \sin^2 G, \quad (7)$$

V_h and V_v being, respectively, the horizontal and vertical velocities of the P-waves. As can be seen from Eq. (6), in (Málek, 1997), the rock massif in the area of the MAYRAU Mine was found to be strongly anisotropic as regards velocity.

The analysis of the distribution of rock-burst foci, with the goal given in the heading to this paper, depends on determining the positions of these foci as accurately as possible. Satisfying this condition essentially depends on determining the objective values of the velocity parameters of P- and S-waves, and of the variations of these values, if required, over the interval of time given above. The different values of the velocities (4), (5) as well as the observed strong velocity anisotropy of P-waves (6) prompted the author to conduct an independent investigation of the velocity model of the mining area in question. For this purpose, the author employed an extensive set of onset-time data obtained within the scope of the operation of the seismic network at the Mayrau Mine in the years 1995 through 1997. As a tool convenient for this investigation, the author chose the methods of the 1st group, referred to above, i.e. various modifications of the classical method. Several theoretical as well as software solutions were thus generated, which enable not only the position of the focus of each recorded burst, but also quantities V_p and V_s of the homogeneous velocity model, and/or the velocity anisotropy of the rock massif to be derived. Various accuracies in measuring the onset times of P- and S-waves, i.e. their various weights, were also incorporated in the solutions.

The next paragraph provides an overview of these methods, together with their theoretical foundations. Since theoretically this involves the standard use of parametric adjustment, the principles of which are generally known from the calculus of observations (Bohm, 1962), only the observation equation, derived by linearizing the basic relation between the onset time, the velocity of the seismic wave and the distance of the burst focus from the seismic station, will be given with each solution:

$$t_i = t + V^{-1} [(x - x_i)^2 + (y - y_i)^2 + (z - z_i)^2]^{1/2}; \quad t_i = t + (d_i/V). \quad (8)$$

To be able to understand this equation, as well as the observation equations given below, it is necessary, at this point, to give the list of symbols used and what they stand for.

t_i – the onset time. The time of arrival of a seismic wave at the i -th station of the seismic network, after adjustment.

tp_i – the onset time of the P-wave, after adjustment.

ts_i – the onset time of the S-wave, after adjustment.

t'_i – the "observed" onset time. The time of arrival of a seismic wave at the i -th station of the seismic network, derived from the seismogram.

tp'_i – the "observed" onset time of the P-wave.

ts'_i – the "observed" onset time of the S-wave.

pp – weight of the time observation of the P-wave.

ps – weight of the time observation of the S-wave.

t – focal time, derived by adjustment.

x_i, y_i, z_i – spatial rectangular coordinates of the i -th station of the seismic network.

x, y, z – spatial rectangular coordinates of the burst focus, determined by adjustment with regard to the equation of observations (8).

d_i – direct distance between the burst focus and the i -th seismic station.

V – velocity of the seismic wave propagating homogeneously along direct lines connecting the focus and the network stations. This quantity may also be the object of adjustment.

V_p – P-wave velocity

V_s – S-wave velocity

q – velocity anisotropy which may be the object of adjustment

V_h – horizontal velocity of seismic waves

V_v – vertical velocity of seismic waves

G_i – zenith distance of the line connecting the burst focus and the position of the i -th seismic station

t_0 – approximate focal time

x_0, y_0, z_0 – approximate values of the spatial coordinates of the burst focus

V_0 – approximate velocity of the seismic wave

V_{p0} – approximate P-wave velocity

V_{s0} – approximate S-wave velocity

q_0 – approximate velocity anisotropy

n – number of stations of seismic network

m – number of observed times entering adjustment

In all the formulae given, the following will apply:

$$t = t_0 + \Delta t, \quad (9)$$

$$x = x_0 + \Delta x, \quad (10)$$

$$y = y_0 + \Delta y, \quad (11)$$

$$z = z_0 + \Delta z, \quad (12)$$

$$V = V_0 + \Delta V, \quad (13)$$

$$V_p = V_{p0} + \Delta V_p, \quad (14)$$

$$V_s = V_{s0} + \Delta V_s, \quad (15)$$

$$q = q_0 + \Delta q, \quad (16)$$

$$d_{0i} = [(x_0 - x_i)^2 + (y_0 - y_i)^2 + (z_0 - z_i)^2]^{1/2}, \quad (17)$$

$$v_i = t_i - t'_i, \quad (18)$$

$$vp_i = tp_i - tp'_i, \quad (19)$$

$$vs_i = ts_i - ts'_i. \quad (20)$$

All the symbols for quantities beginning with the letter Δ represent small final differences of the approximate values of the appropriate quantities with respect to their values derived by adjustment, and symbols v_i , vp_i and vs_i represent the residuals of the observed onset times.

2.1. LOS

The heading of this paragraph indicates a fundamental localization method, used hereinafter, which leads to the adjustment of unknowns T , x , y , and z , the P- and S-wave velocities, V_p and V_s , respectively, being known, if some of the times, tp'_i , as well as ts'_i , have been determined. To be able to use this method, at least 5 such times are required, and these will then enable at least $m = 5$ observation equations to be compiled; some of them may refer to P-waves,

$$vp_i = \Delta t + ap_i \Delta x + bp_i \Delta y + cp_i \Delta z + lp_i, \quad (21)$$

and some to S-waves,

$$vs_i = \Delta t + as_i \Delta x + bs_i \Delta y + cs_i \Delta z + ls_i, \quad (22)$$

In the following equations:

$$\begin{aligned} ap_i &= (x_0 - x_i)/(V_p d_{0i}), & as_i &= (x_0 - x_i)/(V_s d_{0i}), \\ bp_i &= (y_0 - y_i)/(V_p d_{0i}), & bs_i &= (y_0 - y_i)/(V_s d_{0i}), \end{aligned} \quad (23)$$

$$\begin{aligned} cp_i &= (z_0 - z_i)/(V_p d_{0i}), & cs_i &= (z_0 - z_i)/(V_s d_{0i}), \\ lp_i &= t_0 + (d_{0i}/V_p) - tp'_i, & ls_i &= t_0 + (d_{0i}/V_s) - ts'_i, \end{aligned} \quad (24)$$

If the onset times of P- and S-waves are measured, it is sufficient for three seismic stations (e.g., tp'_1 , tp'_2 , tp'_3 , ts'_2 , ts'_3) to be operative to be able to derive the position of the burst focus.

If these times are not measured at all for any one type of seismic wave (in the case of the Mayrau network S-waves were not processed at all during the whole of 1995) at least 5 stations have to be operating in the seismic network ($i = 5$) if $m = 5$ is to be achieved.

If different accuracies, defined by the above weights, are assigned to the observed times tp'_i and ts'_i , minimum condition (3) will be defined as

$$\sum_{i=1}^n (vp_i vp_i pp + vs_i vs_i ps) = \min . \quad (25)$$

As is known from the calculus of observations, in this particular case the adjustment leads to the solution of four linear equations in unknowns Δt , Δx , Δy and Δz . If the approximate values of unknowns t_0 , x_0 , y_0 , z_0 are sufficiently different from their most probable values t , x , y , z , the calculated Δt , Δx , Δy , Δz are used to improve the accuracy of these approximate values with respect to Eqs (9)–(12), and the solution is then repeated. This procedure forms one step of the iteration cycle which has to be repeated until the absolute values of unknowns Δt , Δx , Δy and Δz are below certain limits, set in advance. If these limits have been set incorrectly, i.e. too low, the iteration algorithm may not stop at all. It is then necessary to limit the algorithm to a certain maximum number of iterations. The frequency divergence of the iteration cycle may also be a signal for identifying quite defective observed onset times.

It should be added that the adjustment leads not only to deriving the most probable values of unknowns t , x , y and z , but also to deriving their accuracy. This accuracy is characterized by the mean errors mt , mx , my and mz , derived with the aid of the unit mean error of the observed quantities, m_0 , i.e. with the aid of the mean error of the observed onset times of the P- and S-waves, which, in this case, can be determined from the relation

$$m_0^2 = (m - \nu)^{-1} \sum_{i=1}^n (vp_i vp_i pp + vs_i vs_i ps) \quad (26)$$

where ν is the number of adjusted unknowns. In this particular case, $\nu = 4$. The definition formulae for the mean errors, mt , mx , my , mz , will not be given here, because they are generally known from the appropriate parts of the calculus of observations.

2.2. LOSV

The heading of this section designates another modification of the classical localization method which leads not only to the adjustment of quantities t , x , y and z , but also of velocities V_p and V_s . As indicated in the previous section 2.1, this method will require at least 7 observed onset times of seismic waves to be known, containing the onset times of P- and S-waves alike. The observation equations, subject to minimum condition (25), will in this case read:

$$vp_i = \Delta t + ap_i \Delta x + bp_i \Delta y + cp_i \Delta z + dp_i \Delta V_p + lp_i , \quad (27)$$

$$vs_i = \Delta t + as_i \Delta x + bs_i \Delta y + cs_i \Delta z + es_i \Delta V_s + ls_i , \quad (28)$$

where

$$\begin{aligned} ap_i &= (x_0 - x_i)/(V_{p0}d_{0i}), & as_i &= (x_0 - x_i)/(V_{s0}d_{0i}), \\ bp_i &= (y_0 - y_i)/(V_{p0}d_{0i}), & bs_i &= (y_0 - y_i)/(V_{s0}d_{0i}), \end{aligned} \quad (29)$$

$$\begin{aligned} cp_i &= (z_0 - z_i)/(V_{p0}d_{0i}), & cs_i &= (z_0 - z_i)/(V_{s0}d_{0i}), \\ dp_i &= -(d_{0i}/V_{p0}^2), & es_i &= -(d_{0i}/V_{s0}^2), \\ lp_i &= t_0 + (d_{0i}/V_{p0}) - tp'_i, & ls_i &= t_0 + (d_{0i}/V_{s0}) - ts'_i, \end{aligned} \quad (30)$$

In this case the adjustment leads to the solution of 6 normal equations, and is again carried out iteratively as mentioned above. If the observed quantities do not contain the onset times of a particular type of wave, the equations of observations (27), or (28) do not apply, and the appropriate term, containing the small change of the velocity of the absent waves, in the remaining equations of observations is eliminated. The number of normal equations then reduces to 5. In treating the burst foci, recorded at the Mayrau Mine, one of these options occurs frequently (no S-wave reading). In the following parts of the paper, therefore, the symbol LOSP will refer to the modification of the LOSV method when no S-waves were recorded.

The accuracy of the adjusted unknowns is again characterized by the mean errors mt , mx , my , mz , mV_p and mV_s , derived with the aid of the unit mean error of the observed onset times, defined by Eq. (26) for $\nu = 6$ in the case of the LOSV method, and for $\nu = 5$ in the case of the LOSP modification.

If the LOSV method is used, it is usually convenient to characterize the velocity model obtained by parameter k , defined as the ratio of velocities of both wave types:

$$k = V_s/V_p. \quad (31)$$

Generally speaking, as regards the application of this method it should be pointed out that the position of the burst focus is derived from velocities V_p and V_s , determined simultaneously. If the observed times, tp' and ts' , are subject to larger errors, these velocities may take unacceptable values and throw doubt on the localization in question. The method is thus used to study only singular cases, when an individual investigation of velocities is required, or to determine the average values of these velocities within a particular set of shocks. This method is then used for a purpose similar to that for which the LOTV method, described below, is used. The actual localization of the shock foci is then carried out using the LOS method into which the average values of velocities of both types of seismic waves are introduced.

2.3. LOSI

The modification of the classical localization method designated LOSI rests in adjusting all four fundamental unknowns, t , x , y , z , and the unknown velocity anisotropy, q . In defining quantity q , it is assumed that the horizontal velocity of seismic waves, V_h , is known and that the velocity of seismic waves, V , varies continuously with the zenith distance of their direction, G . For $G = 0$, i.e. in the

direction to the zenith, this velocity takes the unknown value V_v . Quantity q is defined as follows:

$$q = V_v/V_h. \quad (32)$$

The continuous dependence of the seismic wave velocity on angle G , mentioned above, may have various forms. The author of (Málek, 1997) defined this relation by Eq. (7) which, by definition (32), leads to the expression

$$V = V_h [1 + \cos^2 G(q^2 - 1)]^{-1/2} \quad (33)$$

The author of this paper chose to use a different analytical form of this dependence:

$$V = V_h q [1 + \sin^2 G(q^2 - 1)]^{-1/2}, \quad (34)$$

which is the analytical expression of the assumption that the velocity changes from its value V_v to value V_h elliptically. Equation (33) does not have this property.

Incorporating anisotropy of this type, as one of the adjusted unknowns, leads to the following equations of observations in which the horizontal P-wave velocity is designated V_p , and the horizontal S-wave velocity V_s . In the equations of observations, symbol q_0 is used to denote the approximate value of the anisotropy in the sense of Eq. (32), taking the value 1 at the beginning of the iteration procedure, and symbol Δq to denote its unknown difference with respect to its adjusted value:

$$vp_i = \Delta t + ap_i \Delta x + bp_i \Delta y + cp_i \Delta z + dp_i \Delta q + lp_i, \quad (35)$$

$$vs_i = \Delta t + as_i \Delta x + bs_i \Delta y + cs_i \Delta z + ds_i \Delta q + ls_i, \quad (36)$$

with

$$\begin{aligned} ap_i &= (x_0 - x_i)(V_p d_{0i})^{-1} q_0, & as_i &= (x_0 - x_i)(V_s d_{0i})^{-1} q_0, \\ bp_i &= (x_0 - x_i)(V_p d_{0i})^{-1} q_0, & bs_i &= (x_0 - x_i)(V_s d_{0i})^{-1} q_0, \\ cp_i &= (x_0 - x_i)(V_p d_{0i})^{-1} q_0, & cs_i &= (x_0 - x_i)(V_s d_{0i})^{-1} q_0, \\ dp_i &= (x_0 - x_i)(V_p d_{0i} q_0^2)^{-1}, & ds_i &= (x_0 - x_i)(V_s d_{0i} q_0^2)^{-1}, \\ lp_i &= t_0 + (d_{0i}/V_p q_0) - tp'_i, & ls_i &= t_0 + (d_{0i}/V_s q_0) - ts'_i, \end{aligned} \quad (37)$$

and, in view of definition (17), in this particular case

$$d_{0i} = [q_0^2 \{(x_0 - x_i)^2 + (y_0 - y_i)^2\} + (z_0 - z_i)^2]^{1/2}. \quad (38)$$

With a view to condition (25), the adjustment leads to determining unknowns t , x , y , z and unknown q , again by iterative solution of 5 normal equations, as well as to the mean errors of these adjusted quantities, using the unit mean error of the observed onset times, defined by Eq. (26) for $\nu = 5$.

In applying the LOSI method, the question as to which type of wave to include in the adjustment, is considerably problematic. The above equations of observations

are defined for both types of seismic waves. Mostly, however, the LOSI method is only applied to P-waves. The final software form of this method enables both types of waves to be included, but also, of course, enables either type of wave to be excluded, or its effect to be completely suppressed by adopting very small weights of the observed onset times of such waves.

As in the foregoing localization procedures, the accuracy of the adjusted unknowns is characterized by the mean errors mt , mx , my , mz , mq , derived with the aid of the unit mean error of the observed onset times, defined by Eq. (26) for $\nu = 5$.

2.4. LOTV

This designation will hereinafter be used to denote the method leading to the "tomographic" velocities of both seismic wave types, derived by applying the LOS method. As already mentioned, the speed with which the computer deals with the LOS method is high (on a PC 486, 66 Mhz, one solution per approx. 0.005 s). This can be conveniently exploited to determine the most probable values of velocities V_p and V_s within a particular definition set containing a total of N_0 burst phenomena. This involves a very simple method based on the approximate values of both velocities being known quite well.

Around these approximate values as centre values, two intervals are constructed of convenient size, with limits $V_{p\min}$, $V_{p\max}$, $V_{s\min}$, $V_{s\max}$, sufficiently remote from the approximate values. Convenient steps, kV_p and kV_s , providing discretely stepped values of both velocities from minimum to maximum, are then chosen for both intervals. The step is chosen with regard to the accuracy of the results required. $N = N_p \times N_s$ possible combinations of the step velocity values are thus created, where

$$N_p = [(V_{p\max} - V_{p\min})/kV_p] + 1, \quad (39)$$

$$N_s = [(V_{s\max} - V_{s\min})/kV_s] + 1. \quad (40)$$

For each of these N combinations, an average unit mean error, ms , of the observed onset times is then derived using the N_0 mean errors m_0 , which are obtained from the LOS program for N_0 shock phenomena in the treated set. A combination of velocities V_p and V_s is then sought such that its mean error ms is minimum.

The principle of the method is illustrated in Fig. 4 which shows the block diagram of the algorithm described above. The required solution, i.e. the optimum values of both velocities, V_{p_e} and V_{s_e} , as well as the minimum value of the average unit mean error, m_e , are shown in the boldly framed block. This mean error is a general characterization of the accuracy of the computation.

The accuracy of the optimum average velocities, V_{p_e} and V_{s_e} , is characterized by mean errors mV_p and mV_s , respectively. These are derived from the N_0 velocity values obtained from processing the definition set of N_0 shocks, specifically with respect to the phase of the iteration cycle in which the minimum value of mean error m_e is achieved.

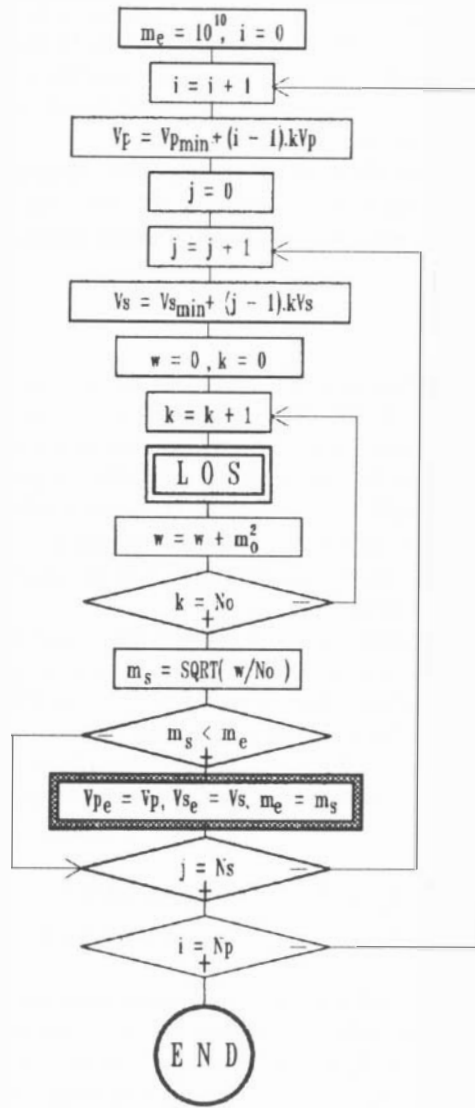


FIG. 4. Block diagram of the LOTV method

As the LOSV method, this method is used only to investigate the velocity model which characterizes a particular set of shocks.

3. INVESTIGATION OF THE VELOCITY MODEL

To be able to derive the objective positions of shock bursts in a given rock massif, it is necessary to determine the most probable values of velocities V_p and V_s of both

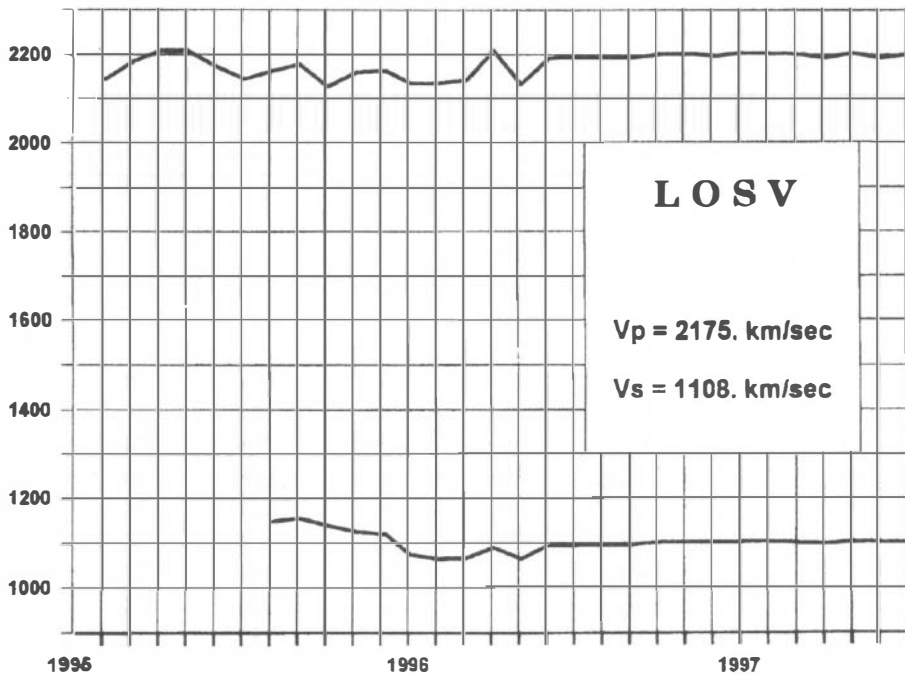


FIG.5. Results of investigating the velocity model using the LOSV method

types of seismic waves. In view of the mining operations being carried out in this rock massif, it is necessary to assume that its mechanical and physical properties may change and, consequently, that the values of both of these velocities, as well as their dependence on the direction of seismic rays, may vary with time and position.

These assumptions led the present author to investigate the values of velocities V_p and V_s , and of velocity anisotropy q , for all rock bursts recorded between 1995.0 and 1997.3, and to identify the time variations of both velocities, if any.

The time unit for this investigation was taken to be 1 month. Within the scope of this unit, representative velocities V_p and V_s were in each case derived using the LOSV and LOTV methods described above. In applying the LOSV program, these representative velocities were derived as the average values of the velocities obtained by applying this program to the separate bursts, recorded within the given month. The sets of time data for the bursts within one month then served to derive the "tomographic" values of both velocities using the LOTV program. The appropriate results are given in Tabs 1 and 2, as well as in Figs 5 and 6.

Table 3 gives the results of investigating the velocity anisotropy using the LOSI program.

These tables and figures clearly indicate, at first glance, that the velocity model may only be investigated using the time data for the bursts generated approximately up to the middle of April 1996. Thereafter, the evaluation procedure of

TAB. 1. Results of investigating the velocity model using the LOSV method

LOSV								
time	number		m_0 [sec]	V_p [km/sec]	mV_p [km/sec]	V_s [km/sec]	mV_s [km/sec]	k
	P	S						
1995, 1	356	—	0.0083	2144.	144.	—	—	
, 2	233	0	0.0083	2185.	151.	—	—	
, 3	145	0	0.0083	2209.	145.	—	—	
, 4	109	0	0.0082	2209.	109.	—	—	
, 5	201	0	0.0088	2173.	136.	—	—	
, 6	135	0	0.0090	2145.	158.	—	—	
, 7	170	5	0.0092	2163.	165.	1148.	19.	0.537
, 8	192	4	0.0093	2178.	154.	1154	58.	0.530
, 9	159	30	0.0083	2188.	148.	1138	74.	0.520
,10	115	36	0.0076	2160.	127.	1125.	59.	0.520
,11	144	22	0.0087	2164.	141.	1118.	50.	0.516
,12	53	51	0.0074	2185.	153.	1073.	50.	0.499
1996, 1	118	115	0.0082	2185.	179.	1064.	76.	0.486
, 2	169	169	0.0074	2141.	193.	1066.	84.	0.500
, 3	127	126	0.0081	2210.	157.	1089.	78.	0.492
mean values				2176.	150.	1108.	60.	0.511
, 4	126	126	0.0040	2133.	134.	1063.	65.	0.498
, 5	279	279	0.0016	2192.	37.	1094.	17.	0.499
, 6	151	151	0.0013	2194.	42.	1095.	16.	0.499
, 7	125	125	0.0012	2193.	36.	1095.	14.	0.499
, 8	122	122	0.0012	2193.	30.	1095.	12.	0.499
, 9	213	213	0.0011	2200.	36.	1100.	14.	0.500
,10	251	251	0.0011	2201.	34.	1102.	13.	0.500
,11	224	224	0.0011	2197.	39.	1100.	17.	0.501
,12	109	109	0.0011	2204.	39.	1102.	15.	0.550
1997, 1	217	217	0.0009	2203.	37.	1102.	18.	0.500
, 2	177	177	0.0007	2200.	34.	1099.	12.	0.499
, 3	125	125	0.0008	2193.	38.	1097.	11.	0.500
, 4	58	58	0.0007	2203.	34.	1102.	12.	0.500
, 5	70	70	0.0008	2193.	38.	1100.	11.	0.500
, 6	45	45	0.0007	2200.	34.	1099.	12.	0.499
mean values			0.0020	2192.	40.	1095.	22.	0.500

localizing rock bursts was changed, and as such has been used to date. This new procedure does not lead to storing the original observed seismic wave onset times at the separate stations of the network, but to recording times already optimized with regard to the preliminary localization carried out using the original times. This is reflected in the decrease of mean errors m_0 to a value roughly equal to 0.001 ms,

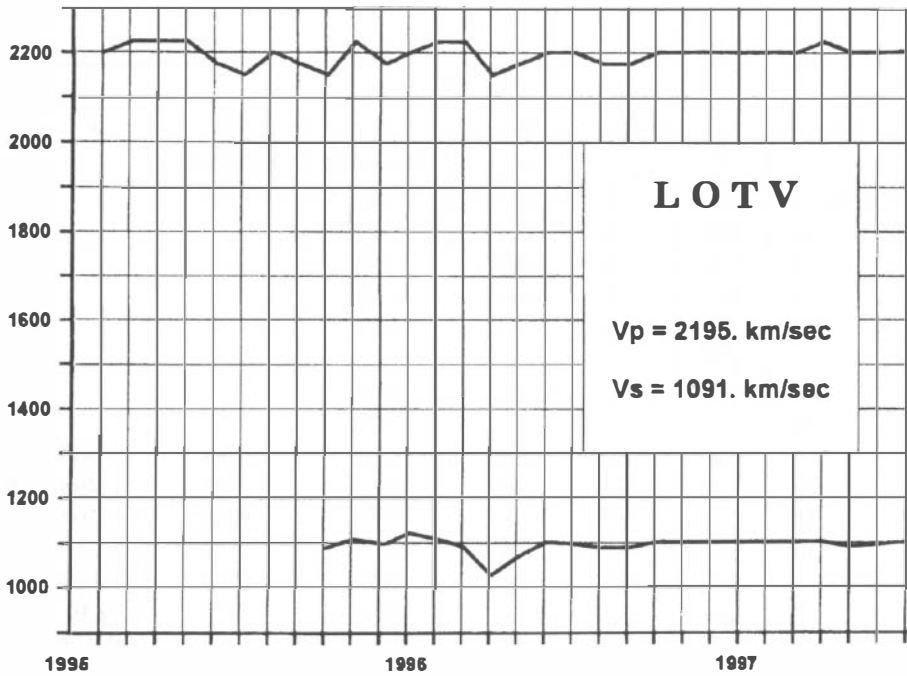


FIG. 6. Results of investigating the velocity model using the LOTV method

which is a quite unrealistic value with regard to the time sampling of seismographic records (4 – 8 ms). This is the reason why the author’s original plan, i.e. to investigate the velocity model within the period of 1995 – 1997.6, could not be completed. Hence, if one considers only the results of investigating the velocity model up to the middle of April 1996, one can draw the following conclusions:

- Variations of P- and S-wave velocities with time cannot be proved.
- The velocities derived from the LOSV and LOTV programs do not display significant differences.
- For the period mentioned above, the following average values can be derived:

	P-waves m/s	S-waves m/s
LOSV program	2175	1108
LOTV program	2195	1091

- The mean value in determining the P-wave velocity is about 150 m/s, i.e. approx. 6% of the velocity of these waves.
- The mean value in determining the S-wave velocity is about 60 m/s, i.e. approx. 5% of the velocity of these waves.
- The anisotropy of ellipsoidal character was studied only for P-waves, and proved to be very small. The average value of ratio (32), q , amounts to about 0.96 with

TAB. 2. Results of investigating the velocity model using the LOTV method

LOTV						
time	number		m_0 [sec]	V_p [km/sec]	V_s [km/sec]	k
	P	S				
1995, 1	356	0	0.0082	2200.	—	
, 2	233	0	0.0094	2225.	—	
, 3	145	0	0.0088	2225.	—	
, 4	109	0	0.0083	2225.	—	
, 5	201	0	0.0093	2175.	—	
, 6	135	0	0.0088	2150.	—	
, 7	170	5	0.0099	2200.	—	
, 8	192	4	0.0090	2175.	—	
, 9	159	30	0.0108	2150.	1088.	0.506
,10	115	36	0.0097	2225.	1108.	0.498
,11	144	22	0.0110	2175.	1096.	0.504
,12	53	51	0.0100	2200.	1122.	0.510
1996, 1	118	115	0.0084	2225.	1108.	0.498
, 2	169	169	0.0067	2225.	1090.	0.49
, 3	127	126	0.0071	2150.	1028.	0.478
mean values			0.0090	2195.	1091.	0.498
, 4	126	126	0.0043	2175.	1070.	0.492
, 5	279	279	0.0023	2200.	1100.	0.500
, 6	151	151	0.0010	2200.	1096.	0.498
, 7	125	125	0.0010	2175.	1088.	0.500
, 8	122	122	0.0010	2175.	1088.	0.500
, 9	213	213	0.0009	2200.	1100.	0.500
,10	251	251	0.0010	2200.	1100.	0.500
,11	224	224	0.0009	2200.	1100.	0.500
,12	109	109	0.0009	2200.	1100.	0.500
1997, 1	217	217	0.0009	2200.	1100.	0.500
, 2	177	177	0.0010	2200.	1100.	0.500
, 3	125	125	0.0010	2225.	1100	0.495
, 4	58	58	0.0009	2200.	1090.	0.495
, 5	70	70	0.0010	2200.	1095	0.498
, 6	45	45	0.0009	2200.	1100.	0.500
mean values			0.0020	2195.	1099.	0.499

a mean error of about 0.01.

– The localization of rock bursts using the LOS program will continue for the seismic wave velocities derived from the LOTV program.

The P- and S-wave velocities, given in the tables for the period after April 1996, only justify the use of the velocities in the

TAB. 3. Results of investigating the velocity anisotropy

LOSI [$V_{hp} = 2200 \text{ km/hour}$]			
time	number P	m_0 [sec]	q
1995, 1	356	0.0083	0.950
, 2	233	0.0087	0.975
, 3	145	0.0083	0.981
, 4	109	0.0082	0.969
, 5	201	0.0088	0.973
, 6	135	0.0090	0.973
, 7	170	0.0092	0.954
, 8	192	0.0093	0.929
, 9	159	0.0083	0.949
,10	115	0.0076	0.978
,11	144	0.0087	0.951
,12	53	0.0074	0.984
1996, 1	118	0.0082	0.963
, 2	169	0.0074	0.970
, 3	127	0.0081	0.899
, 4	126	0.0040	0.965
, 5	279	0.0016	0.991
, 6	151	0.0013	0.993
, 7	125	0.0012	0.992
, 8	122	0.0012	0.992
, 9	213	0.0011	1.000
,10	251	0.0011	1.002
,11	224	0.0011	1.001
,12	109	0.0011	1.001
1997, 1	217	0.0009	1.000
, 2	177	0.0007	1.000
, 3	125	0.0008	1.000
, 4	58	0.0007	1.001
, 5	70	0.0008	1.002
, 6	45	0.0007	1.001

SEISBASE localization program (Buben and Vencovský, 1996).

4. ACCURACY OF LOCALIZING ROCK-BURST FOCI

Determining the accuracy of the positions of burst foci, localized by the LOS or LOSI methods, and determining the distribution of this accuracy in the area of the shaft pillar form an indispensable part of all future deliberations on the origin, distribution and shifting of rock-burst zones as a result of mining operations.

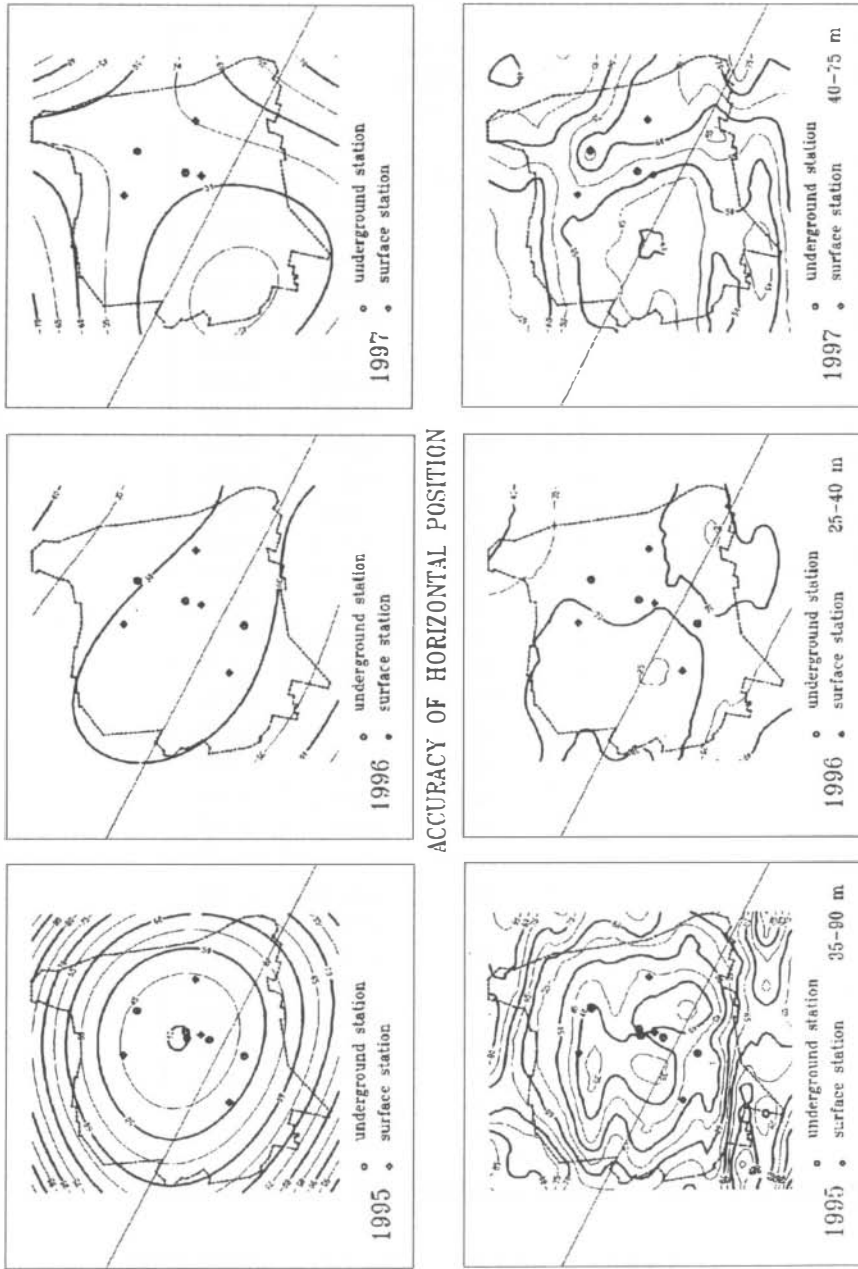


FIG. 7. Estimate of the distribution of accuracy in localizing the epicentre of a rock burst for the three dominant operational conditions of the seismic network

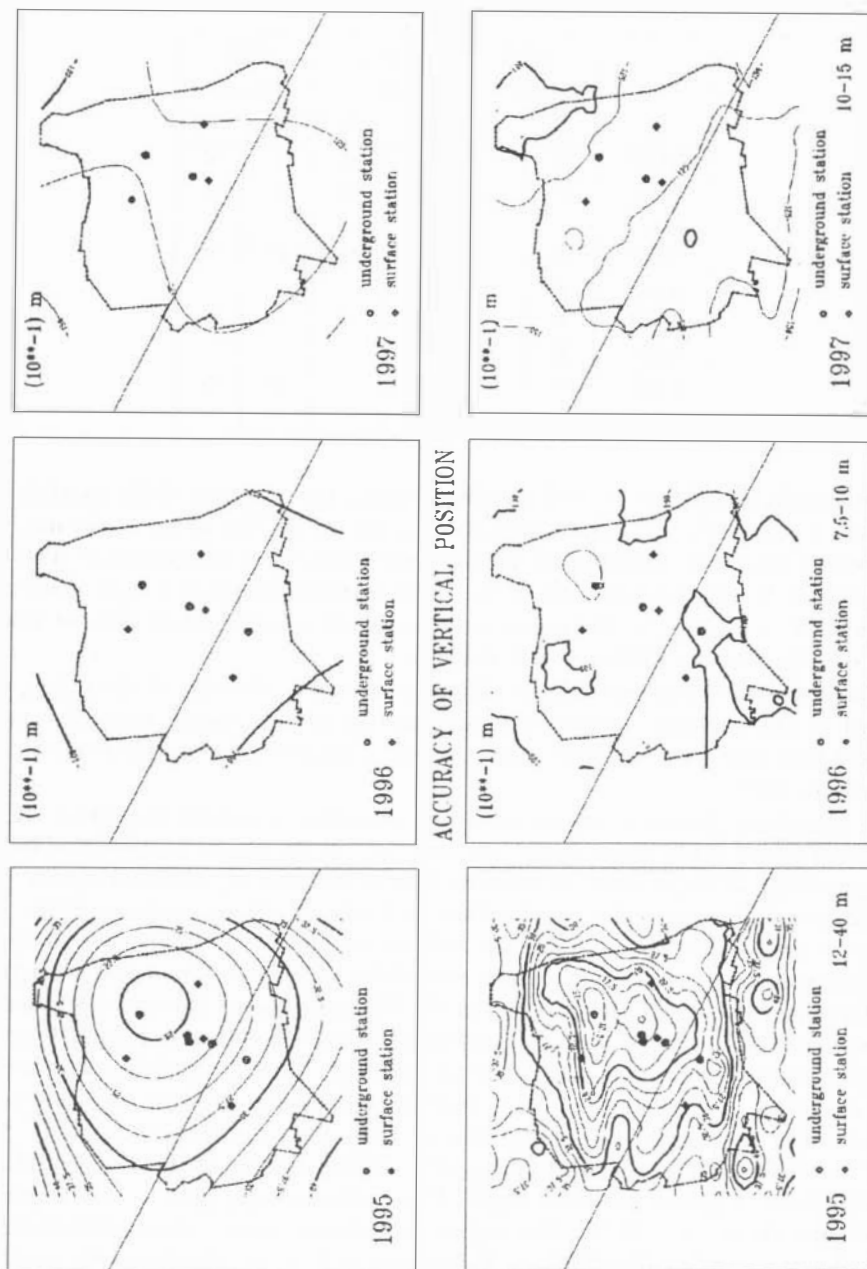


FIG. 8. Estimate of the distribution of accuracy in localizing the height of a rock burst focus for the three dominant operational conditions of the seismic network

TAB. 4.

	1995		1996		1997	
	waves		waves		waves	
	P	S	P	S	P	S
BYT	P	-	P	S	P	S
CEN	P	-	P	S	P	S
DSP	P	-	P	-	-	-
GRZ	P	-	P	S	P	S
KAM	P	-	P	-	-	-
KRY	P	-	P	S	P	S
SED	P	-	-	-	-	-
TRE	P	-	P	-	P	S
PAT	P	-	-	-	-	-

As already mentioned in the foregoing sections, the accuracy of the spatial coordinates, x , y , z , of a particular burst focus is determined by mean errors m_x , m_y , m_z , which represent a concurrent result of the localization computation. The fundamental accuracy characteristic of the whole localization process is, of course, the mean error, m_0 (26), i.e. the mean error in determining the onset time of seismic waves at the stations of the seismic network.

The above distribution of the positional accuracy in the area of the pillar, with regard to the concrete geometrical configuration of the seismic network, can be derived in a number of different ways. An exact analytical procedure is given, e.g., in (Lurka, 1996).

In this study, however, an approximate procedure has been employed. It was based on deriving the mean errors, m_x , m_y , m_z , at the points of simulated bursts, the positions of which were selected to form a horizontally situated square grid. In this particular case, the length of the grid side was 50 m, and ran at the level with the predominating occurrence of rock bursts (about 100 m above the working field) conveniently covering the whole area of the pillar. The simulated onset times of the seismic waves at the stations of the Mayrau seismic network were derived for velocities $V_p = 220$ m/s, $V_p = 1100$ m/s. Each of the times, derived from the simple relation between time, distance and velocity, was then modified with the aid of a generator of random numbers so that the resultant mean error m_0 came out at about 8 ms. This meant varying the times for the P-waves over a range of 0–8 ms, and the times for S-waves over a range of 0–16 ms, the weights introduced into the localization computation in deriving the P-wave times being $pp = 1$, and in deriving the S-wave times $ps = 0.25$. The random-number generator was modified for the Gaussian probability distribution. In support of this investigation, the resultant mean errors m_x , m_y , m_z in the position of each simulated burst were derived as average values of ten independent simulations. Three dimensioned sets of planar point fields, m_x^* , m_y^* , m_z^* of a grid nature were thus obtained. The m_x^* - and m_y^* -sets were then used to create a fourth set, m_{xy}^* , such that each element of this set was determined from the corresponding elements of sets m_x^* and m_y^* as

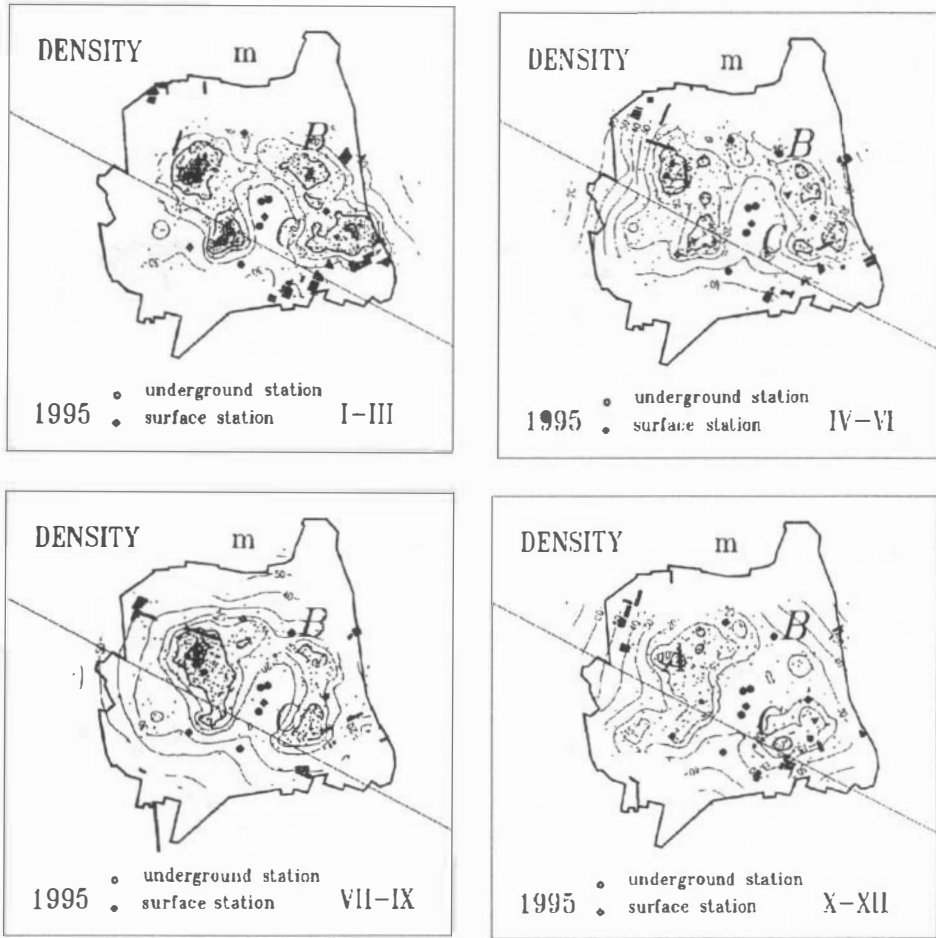


FIG. 9. Quarterly overviews of the distribution of the density of rock burst epicentres in 1995

$$mxy = (mx^2 + my^2)^{-1/2}$$

As can be seen from Fig. 2, the study of the distribution of the burst localization accuracy in the Mayrau network leads to many alternatives which follow from the operational changes in this network. Only the following three alternatives with dominant activities of the separate stations and dominant recording of P- and S-waves will be considered characteristic, see Tab. 4.

The table clearly indicates that the alternative for 1995 was considered without the S-wave reading, although Fig. 2 shows that S-waves were recorded in the last four months of that year. The reason for this is that the number of these recordings was very small. (see Tab. 1).

The results of investigating the accuracy distribution within the chosen square

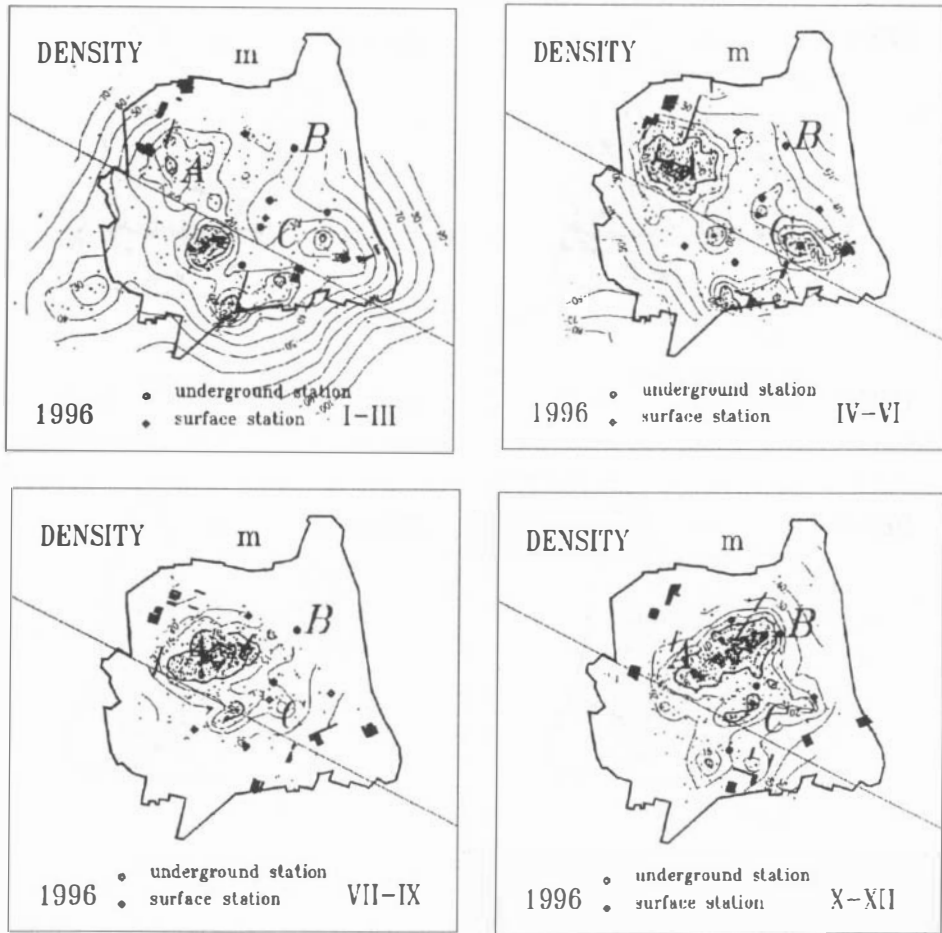


FIG. 10. Quarterly overviews of the distribution of the density of rock burst epicentres in 1996

grid for all three alternative configurations of the Mayrau seismic network are shown in Figs 7 and 8.

Figure 7 shows the surface distribution of the total positional mean error mxy . The analysis has been carried out in the form of digital contour models of the grid type. The digital models of this mean error were constructed from the mxy^* -sets by multiquadric interpolation (Vencovský, 1989) and, consequently they run through all the points of the point mxy^* -field. Their morphologies can be seen from the contours in the lower half of the figure. These contours clearly indicate that the results of investigating the accuracy distribution may, in the given case, be quite complicate, if not confusing. This is due to the actual geometrical configuration and operational situation of the seismic network, as well as to using the approximate

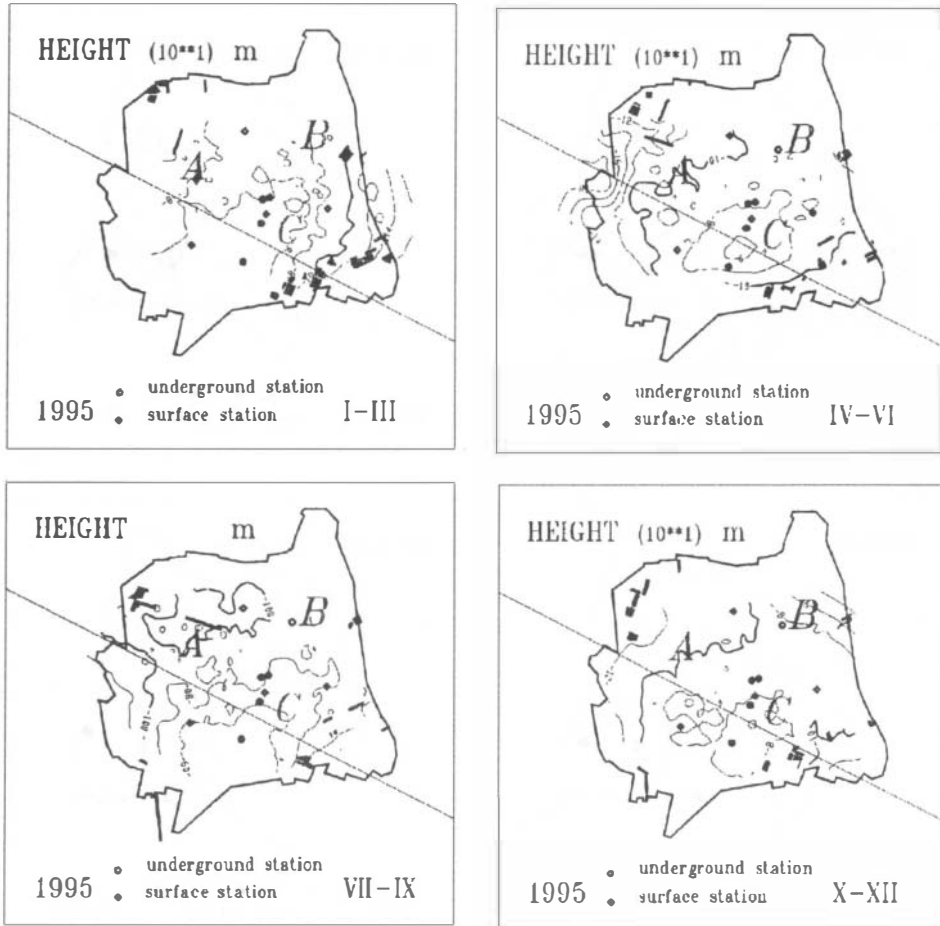


FIG. 11. Quarterly overviews of the distribution of the height of rock burst foci in 1995

procedure described above. To render the representation of this distribution more comprehensible, the mxy^* -sets were also used to construct digital models of bicubic adjustment polynomials which conveniently characterize the height configuration of these point fields with the aid of a mathematical adjustment surface. The contours of these digital models are shown in the upper part of the figure.

The investigation of the surface distribution of the accuracy in localizing the height coordinates of the burst foci by means of the dimensioned point field mz^* was carried out in a similar manner. The results of this investigation are shown in Fig. 8.

Figures 7 and 8 show the following: With regard to the accuracy of localizing the burst foci, using the LOS or LOSI method, the Mayrau seismic network was in the most favourable operational condition in 1996, although, as compared with

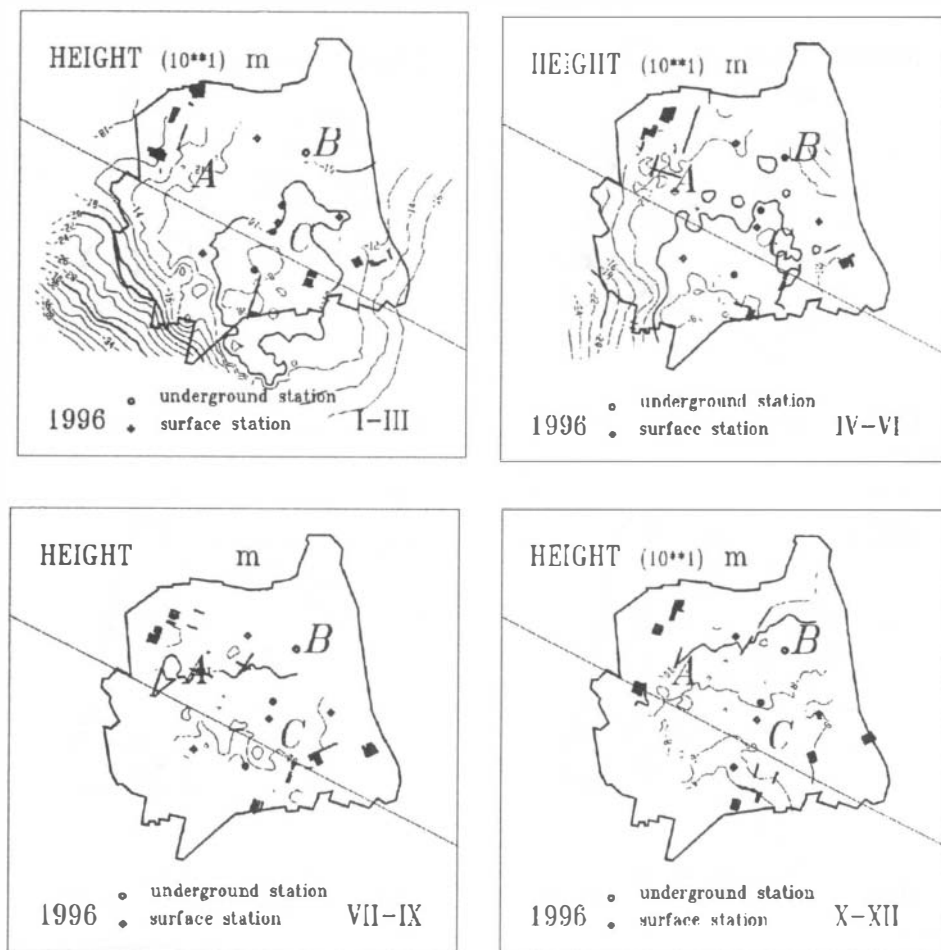


FIG. 12. Quarterly overviews of the distribution of the height of rock burst foci in 1996

1995, 2 seismic stations were not operating. The reason for this is that at most stations P- and S-wave arrival times were being determined that year. In 1997, a third station ceased to operate, which was reflected in a marked decrease of the overall accuracy of the localizations carried out as compared to 1996. In this connection, the Mayrau network's operational condition in 1995 can be labelled as least favourable. Although all the originally installed stations were operating that year, Figs 7 and 8 show the lowest estimate of accuracy and a progressive decrease in accuracy with distance from the geometric centre of gravity of the seismic network. The cause of this is apparently the fact that readings of S-wave arrival times were not made at the network stations practically during the whole year.

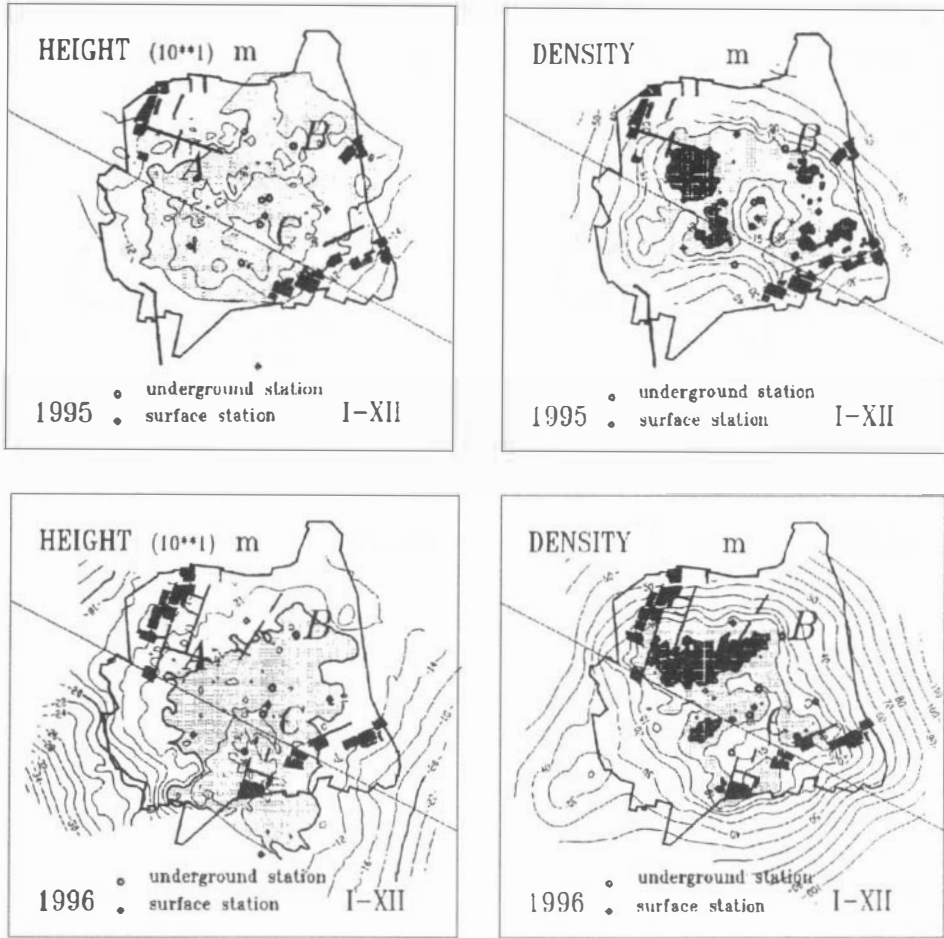


FIG. 13. Annual overviews of the distribution of epicentre densities and foci heights of rock bursts in the years 1995 and 1996

5. RESULTS

The purpose of this study was the position analysis of rock burst foci in dependence on the mining operations being conducted in the shaft pillar of the Mayrau Mine, and deriving facts about the consequences, if any, of these induced rock bursts for the safety of mining operations. In an effort to fulfil this task, the positions of rock burst foci were studied at monthly, quarterly and annual intervals with regard to the height and surface distribution of epicentre densities. A number of graphical documents was thus produced, only some of which will be discussed below. Figures 9-12 refer to quarterly intervals. The density in each case was derived using procedure (Vencovský,1996). In this connection the density is defined as the average distance (m) between the epicentres of the separate rock bursts. Figure 13

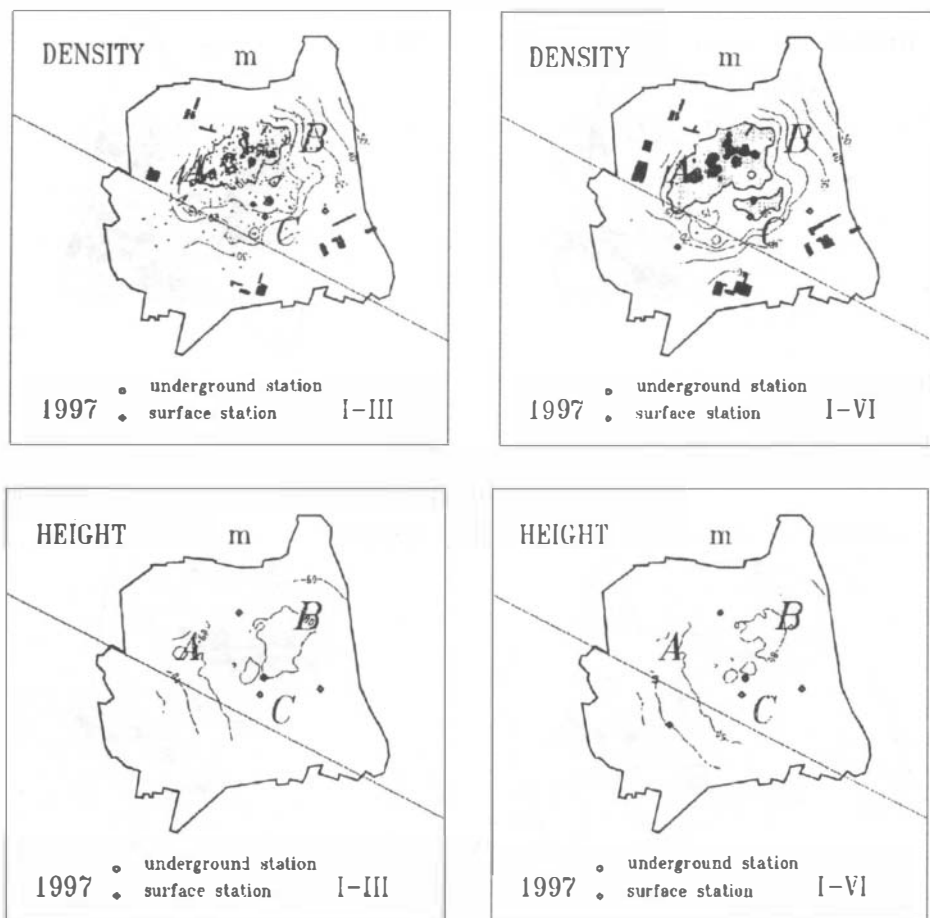


FIG. 14. Overviews of the distribution of epicentre densities and foci heights of rock bursts in 1997

represents an annual overview of both these distributions. Figure 14 supplements these overviews with the development of both distributions in 1997. The following conclusions can be drawn from these figures:

a) Nearly all the rock bursts originate within the shaft pillar. This again points to the hypothesis of brittle failure of the rock massif in the region of the pillar and of the decaying of the burst phenomena in its neighbourhood, already disturbed by old mining operations.

b) The connection between conducting the mining operations and cumulations of burst foci can be identified only very approximately. The calculations carried out to predict the changes in horizontal and vertical displacements for the extent of the mining operations in 1996 and the level at which most of the rock bursts

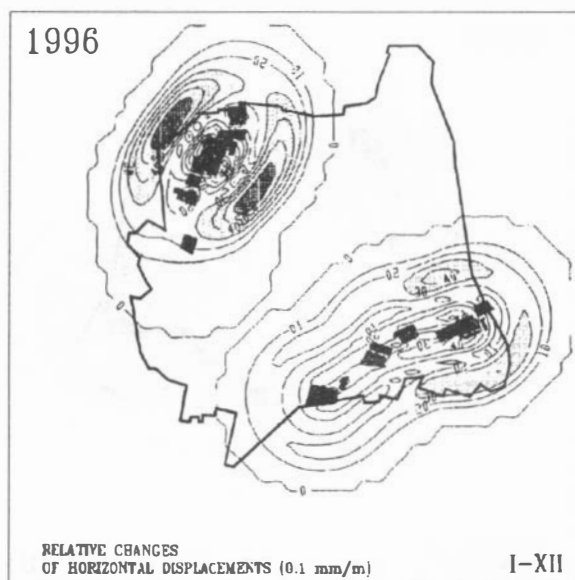


FIG. 15a. Prediction of relative changes (mm/m) of horizontal motions at the level of -100 m for mining operations conducted in 1996. The isolines are dimensioned in tenths of mm/m

occur (80 to 100 m above the stopes) define the region with the maximum values of these changes (Figs 15a, 15b) with the exception of the regions with dominant foci cumulations. As in 1995, bursts were observed only exceptionally in places with maximum displacements, located outside the boundary of the shaft pillar.

c) As regards position, the rock bursts tend to concentrate in "nests", the centres of which remain stable. The most conspicuous such formation is the region marked with the letter A in the figures, which was already identified in earlier papers (Buben and Vencovský, 1996) as the most seismically active region. Similarly, although not to the same extent, bursts were observed to cumulate in the region marked with the letter C. Figures 9 and 13 show very clearly the development of the "nests" in 1995 in the shape of a horseshoe in the vicinity of the mine shaft itself. In that year the mine shaft and the region adjacent to it were affected by rock bursts only very little. In 1996, this phenomenon is not as distinct. A new and quite dominant phenomena in the period from July 1996 to date is the unusually conspicuous concentration of bursts along the line connecting the centre of region A and the centre of the hitherto little active region marked with the letter B. Nearly 65% of all bursts in the said period are distributed along this pronounced line. This gives rise to the presumption that the rock bursts concentrate along some fault, which could have been created as a result of mining operations conducted at the north-west of the pillar and, mainly, as a result of driving mine entries. This is clearly to be seen in

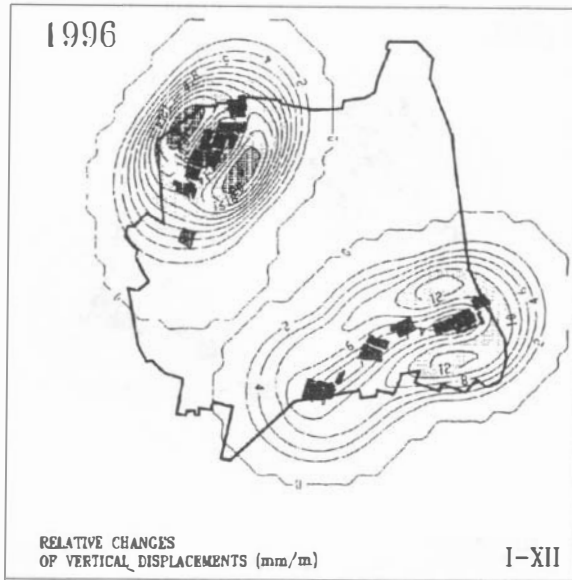


FIG. 15b. Prediction of relative changes (mm/m) of vertical motions at the level of -100 m for mining operations conducted in 1996. The isolines are dimensioned in tenths of mm/m

Fig. 10. However, there is no available geological data to support this presumption.

d) Distribution of rock burst foci in height. The bursts occurring within the pillar are mostly distributed in a horizontally situated region, the lower boundary of which is located at a height of about -100 to -120 m and the upper at about -60 to -80 m. The rock bursts observed at larger depths occur outside the pillar, and apparently have causes other than mining operations within the pillar. The distribution of bursts in height and the fact that the mining operations are conducted at depths of -160 to -180 m lead to the conclusion that the probability the rock bursts will occur directly in the slope regions is very small.

6. CONCLUSION

At the time this study was being completed (September 1997) mining operations were terminated in the MAYRAU Mine, which is to be subsequently liquidated. Consequently, also the seismic network, established in this mine in the past, will cease to operate, and no extension of the results, reported above, will be forthcoming. On the whole, therefore, these results can only be considered preliminary, although they do have their value for the safety of mine operations which are to be continued in several mines of the Kladno Coal Mining Area in the near future.

REFERENCES

- Fischer, T.: 1992, SEISBASE—a PC program for semi-automatic analysis of local network data, *Proc. of XXIII. Gen. Assembly of ESC*, Geophysical Institute AS CR, Prague.
- Růžek, B.: Seismology monitoring, *Acta Montana* **A7** (96), 11–19.
- Málek, J.: 1997, *Interpretace seismogramů z likálních seismických sítí*, Závěrečná práce doktorandského studia, MFF UK Prague, 88 pp. (in Czech)
- Buben, J. and Vencovský, M.: 1996, Focal zones of rockbursts within the shaft pillar of mine KLADNO-2, *Acta Montana* **A10** (102), 179–192.
- Vencovský, M.: 1996, Hustota rozmístění diskretních bodů rovinného pole, *Geodetický a keratografický obzor* **42/84**, 12, 245–248. (in Czech)
- Šílený, J.: 1987, Metoda tomografické lokace důlních otřesů v oblasti Kladna, *Acta Montana* **75**, 65–82. (in Czech)
- Jordan, W. and Eggert, O.: 1920, *Handbuch der Vermessungskunde*, 1. Band, Stuttgart, 620 pp.
- Bohm, J.: 1962, *Vyrovňovací počet*, SNTL Praha, 396 pp. (in Czech)
- Lurka, A.: 1996, A certain new method for seismic network optimization and its consequences, *Acta Montana* **A10** (102), 171–178.
- Vencovský, M.: 1989, *Metody měření a grafického znázornění fyzikálních modelů horninového masivu*, Doktorská disertační práce, ÚGG ČSAV, 298 pp. (in Czech)
- Fischer, T. and Hampf, F.: 1997, SEISBASE—Principles of a Program and Database for Routine Analysis of Data from Local Seismic Networks, Version 4.7, *Acta Montana* **A11** (104), 17–34.

